NASTRAN Based Static CFD-CSM Coupling in FlowSimulator

Bernd Stickan, Hans Bleecke, and Silvio Schulze

Airbus Operations GmbH, Airbusallee 1, 28199 Bremen
{Bernd.B.Stickan,Hans.Bleecke,Silvio.Schulze}@airbus.com
http://www.airbus.com/

Abstract. For high-fidelity fluid-structure interaction simulations different tools are necessary to allow the highest possible accuracy. In this context the data transfer between the aerodynamic surface and the structural model, and the CFD-mesh deformation are the key parameters. This paper shows a methodology to couple different CFD-solvers to the commercial finite element code Nastran. Thereby the coupling scheme can combine different coupling methods, like radial basis function interpolation and structural beam representations, in one coupling matrix. This allows the application of an adequate coupling function for each component of a complex aircraft model. Considering the performance of fluid-structure coupling, the exported spline matrix of a commerical tool is compared to FSAdvancedSplining, a coupling tool integrated into the FlowSimulator software environment. Additionally an update to CFD-mesh deformation with radial basis function interpolation and a strategy for control surface deflection is presented.

Keywords: CFD-CSM-coupling, static aeroelasticity, FlowSimulator, CFD-mesh deformation, control surfaces.

1 Introduction

The objective of this part of the ComFliTe project was to develop a coupling capability to high-fidelity structural models. This is a necessary objective due the high accuracy of nowadays computational fluid dynamics (CFD) solvers. Therefore the fidelity of these codes, which usually solve the Reynolds averaged Navier-Stokes (RANS) equations, is limited by the correct definition of the geometric boundaries.

High fidelity models are not available in the early design phase of aircrafts. Basic structural models, in which the wing is only represented by a beam, are often the starting point for fluid structure coupled simulations, see for example [6]. In a later development stage more complex structural models are used. These models include a detailed representation of the lifting surfaces including control surfaces, but also of other aircraft components like the fuselage, see for example [5]. An example for the need of high-fidelity fluid-structure coupling can be found in [11].

N. Kroll et al. (eds.), *Computational Flight Testing*, Notes on Numerical Fluid Mechanics and Multidisciplinary Design 123,
DOI: 10.1007/978-3-642-38877-4_15,

Here a coupling methodology is presented, which enables the combination of different structural representations in one coupling matrix. Different coupling methods allow to represent aircraft components modeled with differing detail level. Detailed structural models, as well as beam structures and single-point representations can be treated in one method. Detailed FE-models are typically available for the wing, which allow to use radial basis function (RBF) interpolation, while the engines and flap track fairings are only modeled by single mass-points. Therefore only basic rigid-body splines can be used for the coupling of these parts.

If the structural model is used in a high detail level, the size of the coupling matrix will get an issue in terms of performance and memory consumption. On account of this a comparison of an exported spline matrix and FSAdvanced-Splining, a fluid-structure-interaction (FSI) tool in the FlowSimulator software environment, is presented.

Afterwards an update to the mesh deformation module is presented, which enables to represent the exact deflections for every CFD surface grid node, which are delivered by the coupling matrix. Performance limitations dot not allow to use all points as input for the basic radial-basis-function based mesh deformation method.

Then the FSI-loop to compute the static elastic equilibrium is described and the application to an industrial model is presented.

Finally a strategy how to couple and deflect control surfaces is shown. Therefore a possible gapless representation by means of different coupling domains and a chimera-mesh representation is shown.

2 Methods

This section describes the bricks, which are combined to a fluid-structure interaction loop in Section 3. Most of the tools are part of the FlowSimulator software environment, see [7].

2.1 CFD-Solvers: TAU and elsA

Two different CFD-solvers are available within the FlowSimulator environment: The DLR-TAU-code, see [4], and ONERA's elsA code, see [3]. The major difference between the solvers is the used CFD-grid type. The TAU-code uses unstructured CFD-grids, while the elsA-code uses block-structured grids. Both codes solve the RANS-equations, but also more turbulence resolving methods like Detached Eddy Simulations (DES) or Large Eddy Simulation (LES) are available. The discretization is done by finite-volume method with either upwind or centered schemes. Scalar or matrix dissipation is applied to stabilize the discretization and Runge-Kutta or backward Euler integration method is used for the pseudo-time stepping. Multigrid techniques are used for convergence acceleration.

2.2 Structural Solver: Nastran

To create and solve the structural finite element equation system, the commercial MSC Nastran software is used, see [9]. This Computational Structural Mechanics (CSM) tool contains different solution sequences including static linear and nonlinear structural solutions. This is the only brick, which is not part of the FlowSimulator environment, but the, compared to the CFD-domain, low number of degrees of freedom and therefore small data exchange packages are no bottleneck in the overall process.

2.3 Fluid-Structure Coupling

Coupling Methodology The coupling method allows to combine different interpolation methods for different model components. For the case of complex structural models with differently resolved components, this is a very important feature for fluid-structure coupling. Therefore the structural and aerodynamic domain is spitted into several domains. These domains can be components, or further divided components to increase the numerical performance of certain interpolation methods.

The general usage of the interpolation matrix $\mathbf{G}_{\mathrm{CFD,FEM}}$ is the interpolation of the 6 degree-of-freedom (DOF) structural translational and rotational displacements

$$\mathbf{tr}_{\mathrm{FEM}} = \left[(t_x, t_y, t_z, r_x, r_y, r_z)_1 , ..., ((t_x, t_y, t_z, r_x, r_y, r_z)_{n_{\mathrm{FEM}}} \right]^T \tag{1}$$

to the 3 DOF aerodynamic displacements

$$\mathbf{t}_{\mathrm{CFD}} = \left[(t_x, t_y, t_z)_1 , ..., (t_x, t_y, t_z)_{n_{\mathrm{CFD}}} \right]^T \tag{2}$$

by

$$\mathbf{t}_{\mathrm{CFD}} = \mathbf{G}_{\mathrm{CFD,FEM}} \cdot \mathbf{tr}_{\mathrm{FEM}}. \tag{3}$$

To guarantee virtual work conservation, the transposed spline matrix can be used to transport the aerodynamic forces $\mathbf{f}_{\mathrm{CFD}}$ to the structural surface nodes to get the structural forces and moments $\mathbf{fm}_{\mathrm{FEM}}$:

$$\mathbf{fm}_{\mathrm{FEM}} = \mathbf{G}^T_{\mathrm{CFD,FEM}} \cdot \mathbf{f}_{\mathrm{CFD}}. \tag{4}$$

The general interpolation matrix $\mathbf{G}_{\mathrm{CFD,FEM}}$ can be written as a product of the relaxation and blending matrices $\mathbf{M}_{Relax}$ and $\mathbf{M}_{Blend}$, which regulate the combination of different spline domains, and an interpolation method matrix $\mathbf{M}_{Splines}$:

$$\mathbf{G}_{\mathrm{CFD,FEM}} = \mathbf{M}_{Relax} \cdot \mathbf{M}_{Blend} \cdot \mathbf{M}_{Splines}. \tag{5}$$

The matrix $\mathbf{M}_{Splines}$ contains the different interpolation method matrices:

$$\mathbf{M}_{Splines} = \begin{bmatrix} \mathbf{M}_{Spline\_1} & & & \\ & \mathbf{M}_{Spline\_2} & & \\ & & \ddots & \\ & & & \mathbf{M}_{Spline\_nSplines} \end{bmatrix}. \tag{6}$$

Each interpolation matrix $\mathbf{M}_{Spline\_i}$ may represent a different interpolation method. The matrix $\mathbf{M}_{Splines}$ is not block-diagonal, because certain CFD-nodes are influenced by different spline domains due to overlap regions of size $n_{\mathrm{CFD,Overlap}}$. Therefore the matrix has the dimension $3\,(n_{\mathrm{CFD}} + n_{\mathrm{CFD,Overlap}}) \times 6n_{\mathrm{FEM}}$. The blending matrix $\mathbf{M}_{Blend}$ contains entries to unite these multiple interpolation results for certain CFD nodes to a unique result. Afterwards $\mathbf{M}_{Relax}$ modifies the displacements in the vicinity to intersecting domains to sustain a watertight CFD surface mesh.

It is important to note that all three matices $\mathbf{M}_{Relax}, \mathbf{M}_{Blend}$ and $\mathbf{M}_{Splines}$ are sparse, but the domain matrices $\mathbf{M}_{Spline\_i}$ can also be dense.

The main types of interpolation methods, which are used for the spline domains, are:

- radial basis function interpolation: as surface spline, different core functions
- beam spline: the structural component is represented by a line of nodes
- rigid body spline: the structural component is only represented by one node

Spline Export Method. A commercial tool can be used to create the interpolation matrix $\mathbf{G}_{\mathrm{CFD,FEM}}$ in a preprocessing step. The exported matrix is used directly in the here presented FSI-software for fluid-structure coupling. Although the interpolation matrix is of sparse format, the amount of data of such a matrix can be quite large, especially if radial basis function interpolation methods are used. Therefore the matrix is distributed to the parallel high performance computing context during a fluid-structure interaction simulation.

FSAdvancedSplining. FSAdvancedSplining is a fluid-structure coupling tool in the FlowSimulator environment. The main difference between FSAdvancedSplining and the Spline Export Method consists of the fact, that the interpolation matrix $\mathbf{G}_{\mathrm{CFD,FEM}}$ is not created explicitly. Only the relaxation and blending matrix are created in a preprocessing step, while the entries of the domain matrices $\mathbf{M}_{Spline\_i}$ are created "on-the-fly". To speed up the computation of these entries, the preprocessing contains also preparatory work for each spline domain. The amount of data to be stored is reduced enormously. Furthermore FSAdvancedSplining includes an alternative to the force mapping by transposed interpolation matrix: the locally force and moments conservative nearest-neighbor force mapping.

The two proposed fluid-structure coupling methods will be compared in terms of performance in Section 5.

2.4 CFD-Mesh Deformation: FSDeformation Update

FSDeformation is a CFD-grid deformation tool using radial basis function interpolation. For detailed information about FSDeformation it is referred to [1]. For reasons of computational efficiency, not all input points can be considered in the basic RBF-approach.To eliminate the surface interpolation error of the

RBF-method for the case that the deformation input values are given for all surface point, a correction algorithm is presented. A similar method is described in [10].

The general problem about mesh deformation by RBF-interpolation is that for the RBF-interpolation not all input points, in the context of this paper not all CFD-surface points, can be used, because the computational costs would explode. Therefore a reduction method

$$\widehat{\mathbf{x}_{In}}, \widehat{\mathbf{dx}_{In}} = Reduction\left(\mathbf{x}_{In}, \mathbf{dx}_{In}\right) \tag{7}$$

reduces the input points $\mathbf{x}_{In}$ and their deflections $\mathbf{dx}_{In}$ to the base point and deflection sets $\widehat{\mathbf{x}_{In}}$, $\widehat{\mathbf{dx}_{In}}$. The base points are either distributed equidistantly or selected by algorithms, which try to minimize the RBF-interpolation error for the input points $\mathbf{x}_{In}$. The RBF-interpolation is applied to the volume grid points $\mathbf{x}_{vol}$ by

$$\mathbf{dx}_{vol,RBF} = RBF\left(\widehat{\mathbf{x}_{In}}, \widehat{\mathbf{dx}_{In}}, \mathbf{x}_{VOL}\right). \tag{8}$$

Although the input points $\mathbf{x}_{In}$ are a subset of the volume-points $\mathbf{x}_{VOL}$, the RBF-interpolation will only interpolate the correct deformation to the points selected by the reduction method. The remaining surface points $\mathbf{x}_{In} \setminus \widehat{\mathbf{x}_{In}}$ possess an interpolation error. Since the number of selected base points is usually 2-3 orders of magnitude smaller, most of the CFD-surface points are affected. But since the deformation is available for all surface points, the RBF-interpolation surface result $\mathbf{dx}_{surf,RBF}$, which is the surface point subset of $\mathbf{dx}_{vol,RBF}$, can be used to compute the surface interpolation error $\mathbf{e}_{surf}$:

$$\mathbf{e}_{surf} = \mathbf{dx}_{surf,RBF} - \mathbf{dx}_{In}. \tag{9}$$

This error can be used in a correction step. But it is not possible to correct the surface-points directly, because the thin boundary layer cells of a RANS CFD-mesh would be destructed. Instead a nearest-neighbor correction (NNC) method, which takes all volume nodes into account, is proposed.

For the correction step the nearest surface point $\mathbf{x}_{vol,NN}$ of each volume point $\mathbf{x}_{vol}$ is computed. For each of these surface points the interpolation error $\mathbf{e}_{surf}$ is already defined. To get the volume-point errors $\mathbf{e}_{vol}$, the interpolation error of the surface is mapped to the corresponding volume points. But since the correction step should not influence the good mesh quality from the RBF-interpolation, a blending function depending on the surface-boundary distance $\mathbf{d} = (d_1, ..., d_n) = \mathbf{x}_{vol,NN} - \mathbf{x}_{vol}$ limits it to an area close to the surface to get the final volume mesh deformation $\mathbf{dx}_{vol}$. The blending radii $\mathrm{RZW_{NNC}}$ and $\mathrm{RFW_{NNC}}$ are controlling this blending function

$$blend(d_i) = \begin{cases} 0 & : d_i > \mathrm{RZW_{NNC}} \\ 1 & : d_i < \mathrm{RFW_{NNC}} \\ \frac{\mathrm{RZW_{NNC}} - \mathrm{d_i}}{\mathrm{RZW_{NNC}} - \mathrm{RFW_{NNC}}} & : \text{else} \end{cases} \tag{10}$$

to compute the final deformation

$$dx_{vol,i} = dx_{vol,\mathrm{RBF},i} - blend(d_i) \cdot e_{vol,i}, i = 1, ..., n \tag{11}$$

The correction value of the volume grid points decays linearly in the region where $\mathrm{RFW_{NNC}} < \mathrm{d_i} < \mathrm{RZW_{NNC}}$. Volume points with boundary distance d_i larger than $\mathrm{RZW_{NNC}}$ are not affected by the correction step. The RBF-interpolation method uses the same blending function to limit the RBF-volume-mesh deformation to a certain area. But these radii should be selected an order of magnitude larger than the NNC-radii.

Since FSDeformation is already computing the closest surface points during the computation of the wall distances, which are used for the here not mentioned blending and group weighting, anyway, the additional computation time for the correction step is relatively small. Therefore the good performance and mesh-quality conservation of the deformation module is preserved, but the deficit that a complete surface mesh deformation input cannot be represented in the CFD-mesh is removed. Since the coupling method presented in Section 2.3 computes the deformations for all surface points, this is a very important feature in the context of high-fidelity fluid-structure coupling. See also [8].

2.5 FSTrim

FSTrim is a FlowSimulator trimming module, which is based on the six degrees-of-freedom flight mechanics equations. Therefore it can be used to trim aerodynamic coefficients to target values by modifying certain model parameter, like the angle of attack or the HTP-deflection. It uses a Newton algorithm to minimize an internal target function. The necessary Jacobian matrices are discretized by finite differences.

3 Static Fluid-Structure Interaction Loop

The methods presented in Section 2 are combined to compute iteratively the static equilibrium state for certain aerodynamic target coefficients. The process loop is outlined in Figure 1. The starting point for the solution sequence is the CFD-solver. The diagram includes two loops, one for CFD-CSM-interaction and one for trimming. The trim loop begins after the CFD-CSM loop has reached a certain convergence level. Then the CFD-CSM-loop continues after the trim loop has fulfilled its convergence criterion. When both criteria are fulfilled, the elastically trimmed CFD-CSM solution is achieved.

Furthermore it is shown that the trim module FSTrim computes parameter for the CFD solver like the different angles of attack, but also the control surface deflection angles (c.s. parameter). Depending on trim parameter, the trim loop continues with the CFD-solver, the displacement interpolation or the structural solver. This is necessary since the control surface deflection is handled on the structural node set. Either the structural deflection vector $\mathbf{tr}_{\mathrm{FEM}}$ is modified by a rigid control surface deflection, or input is given to the structural model itself. For example actuator forces or multi-point-constraints (MPCs) can be used to change the position of the control surfaces. Actuator forces represent a force pair of equal magnitude but opposite direction, which is used to extend or shorten

the length of actuator elements. An alternative way to model control surface deflections is provided by MPCs. Both allow to cover control surface deflections in the structural and aerodynamic domain. Additionally geometric consistency is assured. Another attribute of control surface deflections in the structural model is the advantage that the interpolation matrix can be used to take care of possible CFD-grid discontinuities, more details in Section 6.

The technical integration of Nastran into the process is done via file exchange. Either binary or ASCII files are written and read to exchange forces and displacements. The data exchange of all FlowSimulator modules is done in memory.

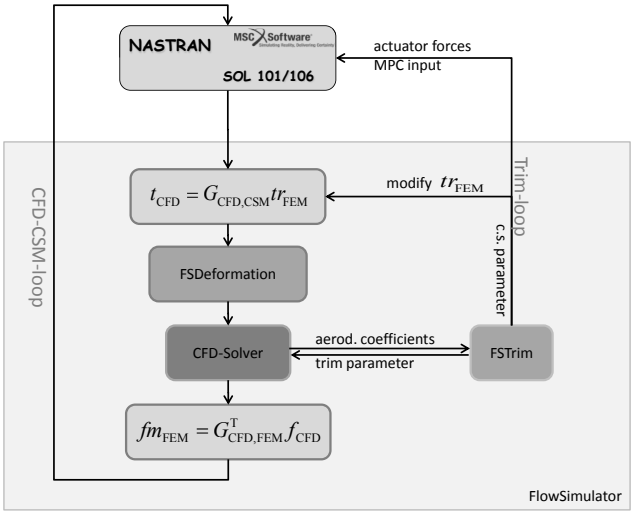

Fig. 1. Static fluid-structure interaction loop with additional trim loop

4 Example Test Case

This section shows the application of the above presented methods to a generic aircraft model. The first step is the fluid structure coupling. Figure 2 shows the coupling domains of the aerodynamic and structural model. Since only radial basis function interpolation and rigid-body splines are used, the structural model is only represented by its nodes. One can also observe, that the lifting surfaces and the fuselage are split into several small domains to increase the performance of radial basis function interpolation. Furthermore the relaxations between the different components are outlined.

The result in terms of bending and torsion of a longitudinal trimmed computation with the parameter Mach-number $Ma = 0.85$, altitude $h = 39.000$ feet lift coefficient $c_{\text{lift}} = 0.47$ and pitching moment $c_{moment,y} = 0.0$ is presented in Figure 3. The structural equations are solved with a static linear solution sequence.

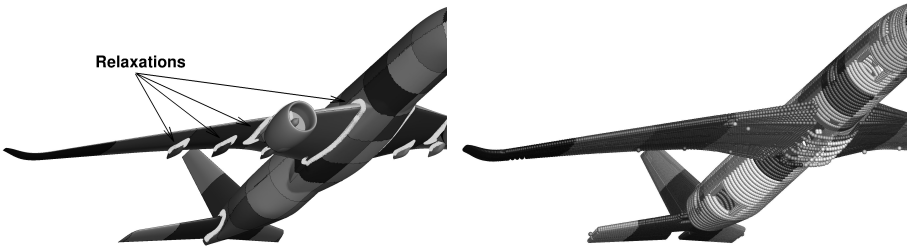

Fig. 2. Fluid-structure coupling example, spline domains visualization: left - CFD model, right - FEM model

As reference to the CFD-CSM-result a standard design tool result is used. The agreement of the two results is very good, only in twist a small deviation can be observed. The two introduced fluid-structure coupling methods did not show differing results.

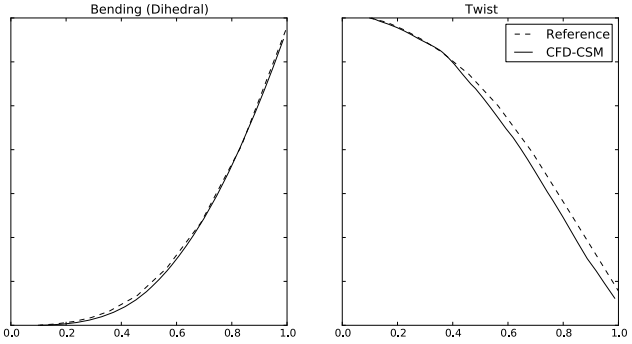

Fig. 3. Bending and twist result of elasticly trimmed simulation

5 Performance Considerations

The fluid-structure coupling example presented in Section 4 is used to compare the performance of the different coupling methods, the Spline Export Method and FSAdvancedSplining. FSAdvancedSplining allows to write input data for the Spline Export Method, therefore the identical interpolation matrices are compared. The number of coupling nodes of the structural model is $n_{\mathrm{FEM}} = 5{\cdot}10^4$ and the number of CFD-surface nodes is $n_{\mathrm{CFD}} = 1{\cdot}10^6$. The models are split into 88 spline domains. The splitting is very important to reduce the computational costs, especially if mainly RBF interpolation is used. The computations have been performed on the same computer system.

Table 1. Performance comparison of the Spline Export Method and FSAdvancedSplining

Method	Spline Export Method	FSAdvancedSplining
Interpolation data file	36GB	0.7GB
Computation start up	1h	5 sec
1 coupling step (CFD → CSM, CSM → CFD)	5s (48 proc)	30s (48 proc)
Total coupling 6 iterations	1h	3min

Table 1 compares the two methods in terms of disk-space/memory needs and the application performance for CFD-CSM-simulations. It is clearly shown that due to the "spline-on-the-fly" approach the interpolation data size is reduced dramatically. The 36GB large matrix from the Spline Export Method is reduced to 0.7GB preprocessing data. For a static FSI-simulation with 6 coupling iterations, the time to load the huge matrix is the main limiting factor. After loading the matrix, the direct parallel product is faster than FSAdvancedSplining. But it takes a large number of iterations until this performance advantage pays off. Additionally the spline matrix demands a lot of main memory on the High-Performance-Computing (HPC) nodes. Furthermore the data handling time, e.g. the time to copy the matrix to a HPC-cluster, is not considered here.

6 HTP and Control Surfaces in Coupling Methodology

This section shows how the coupling methodology can be used for control surfaces.

The first example shows the influence of relaxation in the coupling matrix. For this purpose Figure 4 shows an HTP rotation of approximately -3 degree. It can be observed that the cells below the leading edge are compressed, while the cells above are extended. The shape of the HTP is not affected.

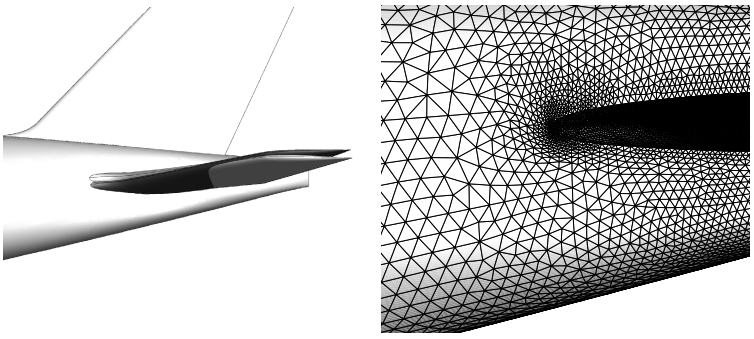

Fig. 4. Approximately -3 degree HTP rotation: left - overview original (white) and deformed (grey) CFD-surface, right - deformed surface mesh

A second example shows how the domain blending can be used for control surfaces. Figure 5, left, shows the coupling of an aileron. Therefore a spline domain for the aileron only has been created. In this case it is important that no structural overlap to the surrounding spline domains is given. Figure 5, right, shows how the spline blending between the domains generates a smooth change over area, which allows to rotate the aileron without disrupting the CFD-mesh.

Both examples show how a 6 DOF trimming can be performed without chimera technique.

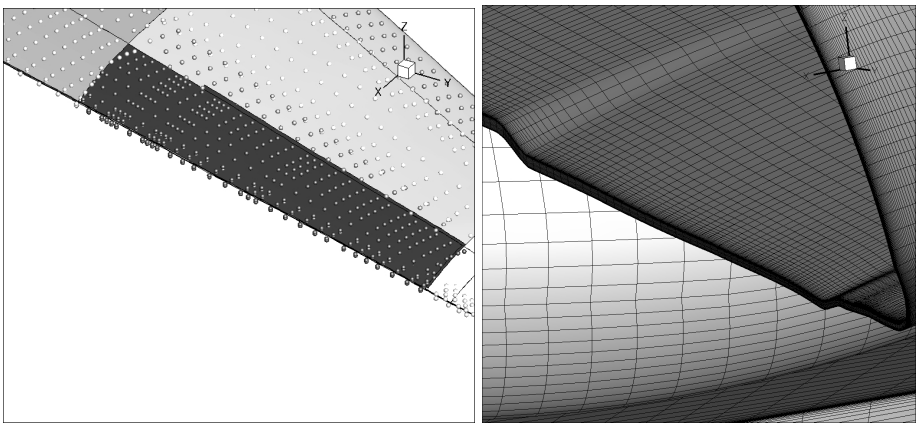

Fig. 5. Gapless aileron representation: left - fluid-structure coupling, spheres identify structural nodes, the underlying surfaces the CFD-mesh-surface, right - deflected aileron

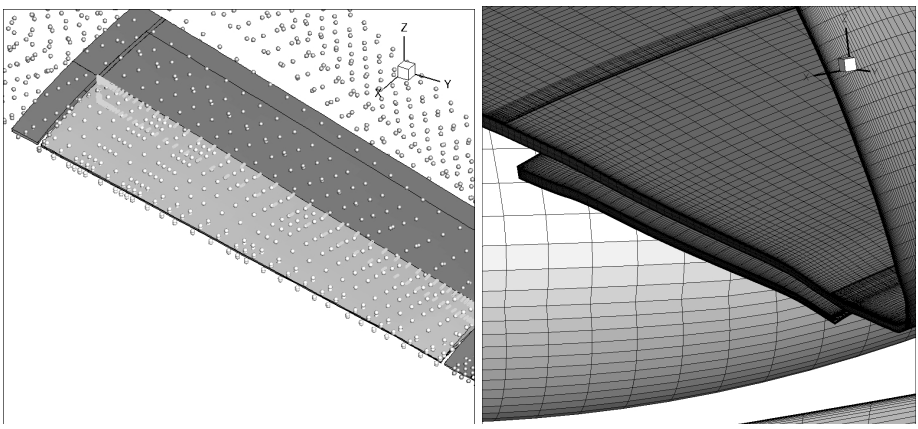

Fig. 6. Chimera aileron representation: left - fluid-structure coupling, spheres identify structural nodes, the underlying surfaces is the CFD-mesh-surface (without chimera background mesh, right - deflected aileron (with chimera background mesh)

Anyway, the coupling method can also be used for chimera meshes. Figure 6 shows the coupling for a chimera aileron. Again the control surface has an own spline domain, but blending or relaxation is only used around the hinge line.

In both cases the spline domains ensure that the aerodynamic forces are mapped to the correct structural components.

7 Conclusion

A fluid-structure interaction process with a multifunctional coupling matrix has been shown. The coupling methodology allows the combination of different interpolation methods, each fitting to the boundary conditions of the used models. Since the spline matrix computes displacements for all surfaces nodes of the CFD-surface mesh, a correction algorithm for mesh deformation with radial basis functions is shown. As application example a complex aircraft example with a very detailed structural and aerodynamic model is presented. For the same test case the benefit of a "spline-on-the-fly" method is shown. It reduces dramatically the necessary amount of stored data for fluid-structure coupling. Finally the flexibility of the coupling approach is underlined by giving some examples about the integration of a trimmed HTP and control surfaces into the coupling process. In [2] more detailed results of the presented FSI-chain are presented.

References

1. Barnewitz, H., Stickan, B.: Improved Mesh Deformation. In: Eisfeld, B., Barnewitz, H., Fritz, W., Thiele, F. (eds.) Management and Minimisation of Uncertainties and Errors in Numerical Aerodynamics. NNFM, vol. 122, pp. 221–246. Springer, Heidelberg (2013)
2. Bleecke, H., Stickan, B.: Industrial comflite applications. In: van der Burg, J.W., Sørensen, K., Kroll, N., Radespiel, R. (eds.) Computational Flight Testing. NNFM, vol. 123, Springer, Heidelberg (2013)
3. Cambier, L., Veuillot, J.-P.: Status of the elsa cfd software for flow simulation and multidisciplinary applicationsa. In: 46th AIAA Aerospace Science Meeting and Exhibit, AIAA 2008-664, Reno, USA (2008)
4. Gerhold, T., Galle, M.: Calculation of complex three-dimensional configurations employing the DLR TAU-code. AIAA Paper 97-0167 (1997)
5. Keye, S.: Fluid-structure-coupled analysis of a transport aircraft and comparison to flight data. In: 39th AIAA Fluid Dynamics Conference, San Antonio, TX, USA (2009)
6. Wiart, G.C.L.: Accounting for wing flexibility in the aerodynamic calculation of transport aircraft using equivalent beam model. In: 13th AIAA/ISSMO Multidisciplinary Analysis and Optimization Conference, AIAA-2010-9135, Fort Worth, TX, USA (2010)
7. Meinel, M., Einarsson, G.: The flowsimulator framework for massively parallel cfd applications. PARA 2010: State of the Art in Scientific and Parallel Computing, Reykjavik (2010)

8. Michler, A., Heinrich, R.: Numerical simulation of the elastic and trimmed aircraft. In: Dillmann, A., Heller, G., Klaas, M., Kreplin, H.-P., Nitsche, W., Schröder, W. (eds.) New Results in Numerical and Experimental Fluid Mechanics VII. NNFM, vol. 112, pp. 109–116. Springer, Heidelberg (2010)
9. MSC. Md nastran 2010 quick reference guide. Technical report, MSC, www.mscsoftware.com
10. Rendall, T.C.S., Allen, C.B.: Parallel efficient mesh motion using radial basis functions with application to multi-bladed rotors. International Journal for Numerical Methods in Engineering (81), 89–105 (2010)
11. Stickan, B., Dillinger, J.: Steady and unsteady simulations of aerostabil windtunnel experiments. In: International Forum on Aeroelasticity and Structural Dynamics (IFASD), Paris (2011)